

Nanostructured ZnO-TiO₂ thin film oxide as anode material in electrooxidation of organic pollutants. Application to the removal of dye Amido black 10B from water

Sana El-Kacemi^{1,3} · Hicham Zazou^{1,2} · Nihal Oturan² · Matthias Dietze³ · Mohamed Hamdani¹ · Mohammed Es-Souni³ · Mehmet A. Oturan²

Received: 12 July 2016 / Accepted: 16 October 2016 / Published online: 25 October 2016
© Springer-Verlag Berlin Heidelberg 2016

Abstract Electrochemical oxidative degradation of diazo dye Amido black 10B (AB10B) as model pollutant in water has been studied using nanostructured ZnO-TiO₂ thin films deposited on graphite felt (GrF) substrate as anode. The influence of various operating parameters, namely the current intensity, the nature and concentration of catalyst, the nature of electrode materials (anode/cathode), and the adsorption of dye and ambient light were investigated. It was found that the oxidative degradation of AB10B followed pseudo first-order kinetics. The optimal operating conditions for the degradation of 0.12 mM (74 mg L⁻¹) dye concentration and mineralization of its aqueous solution were determined as GrF-ZnO-TiO₂ thin film anode, 100 mA current intensity, and 0.1 mM Fe²⁺ (catalyst) concentration. Under these operating conditions, discoloration of AB10B solution was reached at 60 min while 6 h treatment needed for a mineralization degree of 91 %. Therefore, this study confirmed that the electrochemical process is effective for the degradation of AB10B in water using nanostructured ZnO-TiO₂ thin film anodes.

Keywords Amido black 10B · Nanostructured ZnO-TiO₂ · Electrooxidation · Electro-Fenton · Rate constant · Mineralization

Responsible editor: Philippe Garrigues

✉ Mehmet A. Oturan
mehmet.oturan@univ-paris-est.fr

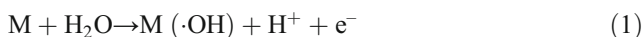
- ¹ Electrochemical, Catalysis and Environment Lab, Science Faculty, Ibn-Zohr University, BO 8106, Dakhla City, Agadir, Morocco
- ² Laboratoire Géomatériaux et Environnement (LGE), EA 4506, UPEM, Université Paris-Est, 77454 Marne-la-Vallée, France
- ³ Institute for Materials & Surface Technology, University of Applied Sciences, Kiel, Germany

Introduction

Dye compounds are of the most obvious indicators of water pollution issued from discharges of colored wastewater effluents. Dyes are largely used in various human activities and in a predominant way in the textile industry (Guivarch et al. 2003; Brillas and Martínez-Huitle 2015). Textile dyes are released in the sewage system during manufacturing or processing operations (Sen and Demirer 2003; Brillas and Martínez-Huitle 2015). As they are mostly composed of persistent organic molecules and not efficiently retained by WWTP, they constitute a major source of environmental contamination. More than 10,000 dyes, with an annual production of 7×10^5 metric tons, are commercialized worldwide (Toh et al. 2003; Senthilkumar et al. 2014). Among them, azo-type compounds represent 60–70 % of dyes used in textile industries (Arslan et al. 2000). About 10 % of dyes used in textile industry are lost in water during dyeing operation. When somehow incorporated into the human body, soluble azo dyes can undergo breaking reactions to form corresponding aromatic amines, which can cause cancer (Mirkhani et al. 2009; Chung 2015). Among them, Amido black 10B (AB10B), which is an amino acid staining diazo dye, applicable to natural and synthetic textile fibers and leather, is widely used in paints, inks, and plastics.

To develop an environmental friendly technology, electrochemical techniques provide good tool for degradation of organic pollutants. The electrochemical advanced oxidation processes (EAOPs) are among advanced oxidation processes and largely used in the treatment of industrial wastewaters (Brillas et al. 2009; Panizza and Cerisola 2009; Oturan 2014; Vasudevan and Oturan 2014; Lee et al. 2015; Shukla and Oturan 2015). EAOPs are based on in situ electrocatalytic

generation of highly powerful oxidizing agent hydroxyl radicals ($\cdot\text{OH}$) that are able to oxidize organic pollutants until mineralization, i.e., transformation of organics to CO_2 , water, and inorganic ions (Panizza and Cerisola 2009; Oturan and Aaron 2014; Rodrigo et al. 2014; de Araujo et al. 2015). One of the most popular EAOPs is the electrooxidation (or anodic oxidation) process in which degradation of the organic pollutants is carried out by $\text{M}(\cdot\text{OH})$ generated on a suitable anode (M) surface from water oxidation according to reaction (1) (Panizza and Cerisola 2009; de Araujo et al. 2014; Panizza et al. 2014). In this process, the electrocatalytic activity of the anode is the main driving force to decolorize the textile effluents. Anodes having high oxygen evolution overvoltage like boron-doped diamond (BDD) film electrodes or mixed metal oxide anodes such as PbO_2 have shown to be more suitable for this process (Martinez-Huitle et al. 2004). The electrooxidation is an attractive process because of its simplicity and its oxidation power leading to removal of organic pollutants and thus leaving non or less toxic residues in the medium (Brillas et al. 2009). The ultimate desirable stage is the complete incineration reaction leading to the mineralization of organics (Brillas and Martinez-Huitle 2011; Rocha et al. 2012).



The oxidation power of the process can be significantly enhanced when using a cathode able to produce H_2O_2 (reaction 2). In the presence of a catalytic amount of ferrous iron, the Fenton reaction (reaction 3) takes place to generate homogeneous $\cdot\text{OH}$ in a system called electro-Fenton process (Brillas et al. 2009; Sirés et al. 2014). The process is electrocatalytic since ferrous iron is regenerated continuously, according to reaction (4), by electroreduction of Fe^{3+} formed in reaction (3). In this case, hydroxyl radicals are produced simultaneously both on the anode surface (heterogeneous $\text{M}(\cdot\text{OH})$) and in the bulk solution (homogeneous $\cdot\text{OH}$) providing a high amount of radicals and a much more oxidation/mineralization power of the process (Oturan et al. 2012; Labiadh et al. 2015; El-Ghenymy et al. 2014).

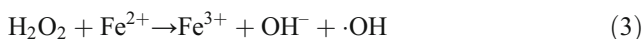
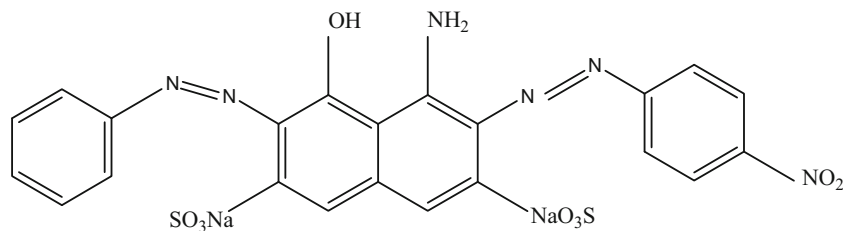


Fig. 1 Structure of dye Amido black 10B



Different processes, such as Fenton oxidation (Sun et al. 2007), adsorption (Tan et al. 2015), and photodegradation (Qamar et al. 2005; Kirupavasam and Raj 2012; Aboul-Gheit et al. 2014) were employed for degradation of AB10B. Moreover, the decolorization of AB10B aqueous solutions using AOPs has been recently reviewed (Hisaindee et al. 2013). But its efficient removal (mineralization) from water has not been investigated. Therefore, the main objective of this work was to optimize the oxidative degradation of AB10B and mineralization of its aqueous solution by EAOPs in aqueous medium using a nanostructured ZnO-TiO₂ thin film anodes on graphite (GrF) substrate, noted GrF-ZnO-TiO₂. For this purpose, the influence of various experimental parameters such as the current density, nature and concentration of the catalyst, and the nature of electrode (anode and cathode) material were investigated. The contribution of the electro-Fenton process to the electrooxidation of AB10B was also studied and discussed.

Materials and methods

Chemicals

Dye AB10B (4-Amino-5-hydroxy-3-[(4-nitrophenyl)azo]-6-(phenylazo)-2,7-naphthalenedisulfonic acid, disodium salt), $\text{C}_{22}\text{H}_{14}\text{N}_6\text{Na}_2\text{O}_9\text{S}_2$, was provided by Carl Roth, Germany. Other chemicals used in this study were as follows: sulfuric acid (H_2SO_4 , 98 %, SDFCL), hydrogen peroxide (H_2O_2 , 35 %, Carl Roth), zinc nitrate hexa-hydrated, ($\text{Zn}(\text{NO}_3)_2 \cdot 6\text{H}_2\text{O}$, Loba Chemie), diethanolamine (DEA ($\text{C}_4\text{H}_{10}\text{NO}_2$, Loba Chemie), titanium (IV) isopropoxide ($\text{Ti}\{\text{OCH}(\text{CH}_3)_2\}_4$, 97 %, Aldrich, Germany), ammonia (NH_3 , 25 %, Roth, Germany), potassium sulfate (K_2SO_4 , Merck, Germany), absolute ethanol (Merck, Germany), sodium sulfate (Na_2SO_4 , Loba Chemie), iron (II) sulfate heptahydrated ($\text{FeSO}_4 \cdot 7\text{H}_2\text{O}$, Loba Chemie), copper (II) sulfate pentahydrated ($\text{CuSO}_4 \cdot 5\text{H}_2\text{O}$, Loba Chemie), and Graphite felt (GrF) (Alfa Aesar, GmbH, Germany). All these chemicals were of analytical grade and were used without further purification. The chemical structure of AB10B used as the target pollutant in this work is given in Fig. 1, which presents the following characteristics: molar mass $616.50 \text{ g mol}^{-1}$, solubility in water at $20 \text{ }^\circ\text{C} \sim 30 \text{ g L}^{-1}$, and

density 1.05 g L^{-1} at $20 \text{ }^\circ\text{C}$. Deionized water was used in preparation and dilution of solutions throughout the work.

Preparation and characterization of graphite felt substrates and thin films

A volume of 50 mL of the binary mixture of H_2SO_4 ($3.0 \times 10^{-2} \text{ M}$) and hydrogen peroxide in a 1:4 ratio was used to clean organic residues of graphite felt (GrF) substrates. This mixture is a strong oxidizing agent which removes most of organic matters. Besides, it hydroxylates GrF surfaces by adding $-\text{OH}$ groups, making them highly hydrophilic. The ZnO thin film was prepared firstly on GrF substrate using 15 mM Zn $(\text{NO}_3)_2 \cdot 6\text{H}_2\text{O}$ dissolved in 50 mL H_2O with stirring. 10 mL of this solution was mixed with 5 μL DEA and then 40 μL NH_3 (25 %) was added to this solution with stirring. Subsequently, GrF substrates were immersed in the mixed solution at room temperature for 2 h. The substrates were then removed from the solution and cleaned ultrasonically with ethanol and subsequently dried at $80 \text{ }^\circ\text{C}$ in the stove for a period of 1 h to obtain GrF-ZnO substrates (Es-Souni 2011).

The second step consisted of preparation of the TiO_2 thin film oxide on GrF substrates covered by ZnO oxide (i.e., GrF-ZnO). The two solutions, named “Sol A” containing 5 mL ethanol (99 %) and 25 μL ammonium hydroxide (25 %), and “Sol B” containing 5 mL ethanol (99 %) and 295 μL titanium (IV) isopropoxide were prepared. Sol A and Sol B were then mixed on magnetic stirring conditions for 20 min. The prepared GrF substrates, GrF-ZnO, were immersed for 30 min in this mixture. Thereafter, they were cleaned with ethanol and dried in an oven at $T = 60 \text{ }^\circ\text{C}$. The samples were then heat-treated at $450 \text{ }^\circ\text{C}$ at the furnace for 1 h in ambient atmosphere. Details of the preparation of TiO_2 are described in our previous article (Es-Souni 2011). The prepared oxides were investigated by X-ray diffraction (XRD) (X’Pert Pro, PANalytical, Holland), and the surface was characterized using a high-resolution scanning electron microscope (Ultra Plus, ZEISS, Germany) provided with energy-dispersive X-ray spectroscopy (EDS).

Analysis of AB10B

Analysis of AB10B solutions was performed using a UV-Vis spectrophotometer (JASCO V-630). The maximum absorbance wavelength (λ_{max}) of AB10B was 617 nm with an absorption equal to 0.152 unit.

Electrochemical system and procedures

Degradation experiments were carried out in a 250-mL undivided glass cell equipped with two electrodes. A GrF-ZnO- TiO_2 composite thin film ($4 \text{ cm} \times 4 \text{ cm} \times 0.2 \text{ cm}$) was used as

anode and a graphite felt piece ($19.5 \text{ cm} \times 6 \text{ cm} \times 0.5 \text{ cm}$) was used as cathode to determine the effect of several physico-chemical parameters on the degradation of AB10B during EAOPs. Experiments were carried out under galvanostatic conditions. A power supply (ELC model AL781N) was used to provide the desired constant current. The pH of the solution was adjusted to three by adding the concentrated sulfuric acid (1 M) or NaOH (1 M). Prior to the electrolysis of the solution, the anode was equilibrated for 30 min at ambient temperature ($20 \pm 1 \text{ }^\circ\text{C}$). The solution was saturated with compressed air at 2.5 L min^{-1} flow rate.

The total organic carbon (TOC) as equivalent of dissolved organics was used to evaluate the mineralization degree of treated aqueous solution. The decrease of solution TOC means the conversion of organic matter present in the solution to CO_2 mainly by $\text{M}(\cdot\text{OH})$ and $\cdot\text{OH}$ generated in the process. TOC measurements were performed in a combustion chamber at $680 \text{ }^\circ\text{C}$ on a Pt catalyst in a stream of pure oxygen using Shimadzu VCSH TOC analyzer equipped with a manual injector. CO_2 formed following the combustion of organic matter was determined by IR spectroscopy placed at the furnace outlet. To avoid the presence of inorganic carbon, samples were acidified by 1 % hydrochloric acid before injection. Each measure was repeated three times, and the result is calculated from the average of the two closest values. Analyses were made by external calibration using standard potassium hydrogen phthalate solution.

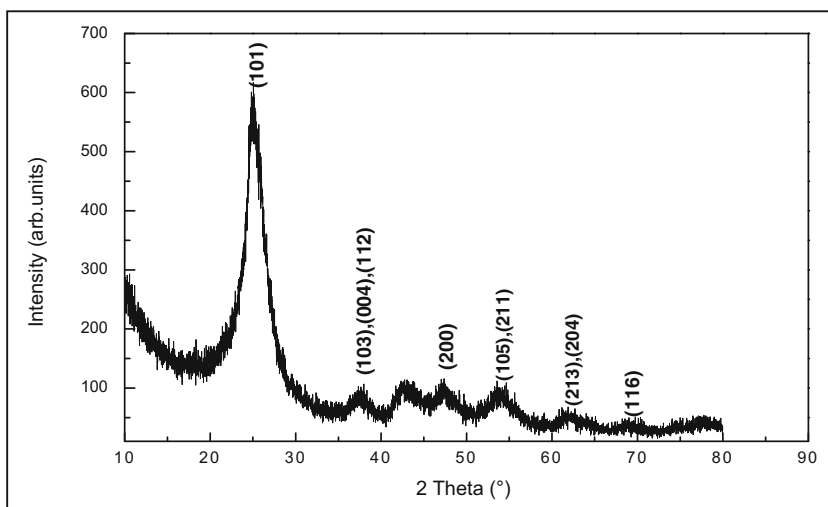
Results and discussion

XRD and SEM characterization of GrF-ZnO- TiO_2 composite films

Figure 2 shows the XRD pattern of GrF-ZnO- TiO_2 composite film annealed at $450 \text{ }^\circ\text{C}$ for 1 h. The spectrum shows the diffraction peaks of TiO_2 at $2\theta = 25^\circ$ (101), $2\theta = 37^\circ$ (103), and $2\theta = 54^\circ$ (105), which are the characteristics of the anatase form of TiO_2 . However, Fig. 2 did not show any diffraction peaks corresponding to the presence of ZnO in the composite film. Thus, ZnO might be in the amorphous form.

The scanning electron microscopy (SEM) of GrF-ZnO- TiO_2 composite film annealed at $450 \text{ }^\circ\text{C}$ for 1 h is shown in Fig. 3a. Formation of a homogeneous thin film on graphite felt substrate is obtained. The films are nanostructured with a mean grain size of 20–30 nm mesoporous and seem to be well adherent to the substrate, filling even the interior of the graphite felt pores. The EDS spectrum (Fig. 3b) shows the presence of both Zn and Ti oxides on GrF. However, XRD of GrF-ZnO- TiO_2 did not produce any diffraction peak for ZnO. Thus, the EDS result substantiates the presence of ZnO in amorphous form in the composite sample.

Fig. 2 XRD pattern of GrF-ZnO-TiO₂ composite film on graphite felt



Effect of the experimental parameters on the degradation of AB10B

Nature of the electrode materials

To evaluate the effect of the nature of the anode, kinetic study of electrochemical degradation of AB10B has been performed with different anodes, such as uncovered GrF, GrF-ZnO, GrF-TiO₂, and GrF-ZnO-TiO₂, using graphite felt as the cathode and results are depicted in Fig. 4. As can be seen on this figure, the better degradation rate of AB10B was obtained with GrF-ZnO-TiO₂ anode, while the non-modified GrF anode provided poorer AB10B concentration decay with an oxidation rate of 35 % of initial AB10B concentration. Better oxidative degradation performance was obtained with GrF-ZnO-TiO₂ composite thin film anode reaching 98 % dye degradation at 70 min electrolysis. Degradation efficiency was slightly lesser in the case of GrF-TiO₂ (96 %) which provides significantly better result compared to GrF-ZnO anode (88 %). These results highlight that the GrF-ZnO-TiO₂ anode provides better degradation performance in electrooxidation of AB10B compared to other tested anodes and therefore it has been chosen for further investigation.

To evaluate the effect of the nature of cathode material, electrooxidation of AB10B solutions was performed using three sets of cathode/anode combination. The worst degradation efficiency of AB10B was obtained when the cathode and the anode are made of untreated graphite felt (GrF/GrF). When the GrF cathode was substituted by the stainless steel (SS) cathode (4 cm × 4 cm × 0.2 cm), only 50 % of AB10B was degraded after 60 min electrolysis time. The combination GrF/GrF-ZnO-TiO₂ provided far the best degradation efficiency achieving total disappearance of the dye at 60 min electrolysis. This result highlights the importance of graphite felt as the cathode in electrooxidation process and the contribution of homogeneous ·OH generated from Fenton reaction (2). SS cathode is not a suitable material for electrogeneration of H₂O₂ and therefore Fenton reaction does not take place to form ·OH. In this case, the electrooxidation of the dye was conducted only by heterogeneous hydroxyl radicals M (·OH) produced on GrF/GrF-ZnO-TiO₂ anode.

Effect of current intensity

The value of the applied current is the main parameter in electrochemical processes since the rate of hydroxyl radical generation is monitored through the reactions (1–4). Therefore, the

Fig. 3 a SEM image. b EDS of GrF-ZnO-TiO₂

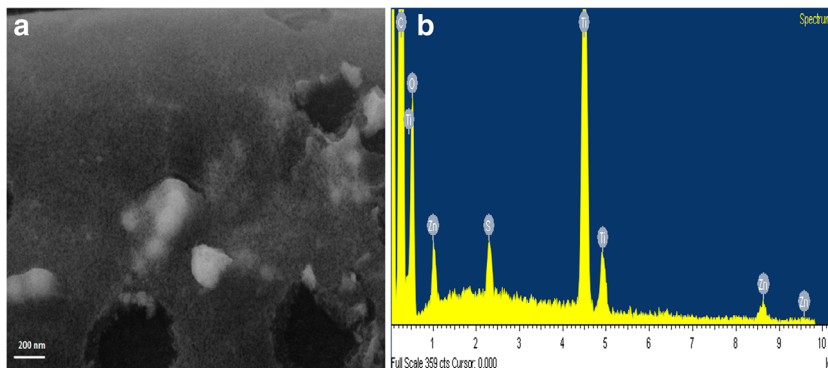
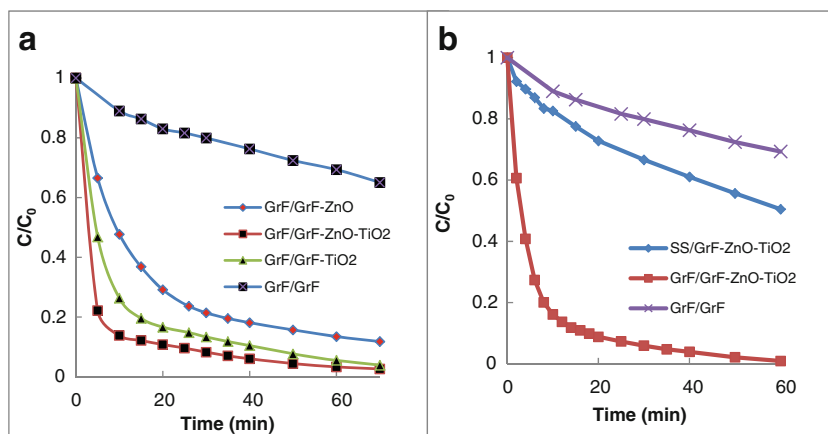


Fig. 4 Effect of the nature of electrode material on the degradation of AB10B. **a** Effect of anode materials. **b** Effect of cathode materials. $[\text{dye}]_0 = 0.12 \text{ mM}$, $[\text{Na}_2\text{SO}_4] = 60 \text{ mM}$, $I = 100 \text{ mA}$, $[\text{Fe}^{2+}] = 0.1 \text{ mM}$, $\text{pH} = 3$, $T = 20 \pm 1 \text{ }^\circ\text{C}$, air flow rate = 2.5 L min^{-1}



effect of current intensity on the electrodegradation of AB10B was assessed and results are shown in Fig. 5. The electrolysis time required for complete disappearance of AB10B was shorter when the applied current values were high. The oxidation kinetics increased with increase of current intensity until 100 mA. Further increase in current did not conducted to a significant enhancement in oxidation efficiency. Thus, the value of 100 mA applied current intensity was chosen as optimal for oxidative degradation of AB10B dye with GrF-ZnO-TiO₂ anode. On the other hand, as can be seen on Fig. 5a, dye concentration decreases exponentially as a function of the time, indicating that the oxidation reaction of AB10B occurred according to a pseudo first-order kinetics (Fig. 5b). The kinetic analysis of data from this figure allowed us to determine the value of the apparent rate constants (k_{app}) versus applied current (Fig. 5). The k_{app} values thus calculated are presented in Table 1. Obtained k_{app} values highlight better kinetic rates for higher applied currents confirming the above discussion.

Effect of catalyst (Fe^{2+}) concentration

To elucidate the role of initial concentration of Fe^{2+} ($[\text{Fe}^{2+}]_0$) as catalyst of electro-Fenton process on the degradation efficiency of AB10B, a series of experiments were conducted without

Fe^{2+} and with different $[\text{Fe}^{2+}]_0$ from 0.06 to 0.5 mM. Figure 6 shows the effect of $[\text{Fe}^{2+}]_0$ on the AB10B concentration decay. In the absence of Fe^{2+} , only 85 % of initial dye was oxidized at 70 min. Degradation efficiency increased in the presence of ferrous iron, but it seems not to be significantly affected in the range of 0.06–0.5 mM—oxidation rate being 98.7, 99.0, and 99.2 % for 0.1, 0.2, and 0.5 mM initial Fe^{2+} concentration, respectively, after 60 min electrolysis. The use of Cu^{2+} ions instead of Fe^{2+} under same operating conditions conducted to 96.3 % degradation of AB10B. Considering these results and the need to remove iron after treatment, the optimal Fe^{2+} concentration was selected as 0.1 mM for the degradation of AB10B dye. This value is in agreement with already published reports (Brillas et al. 2009; Lin et al. 2016).

Effect of other parameters with low influence

The ability of absorption of the dye AB10B on the untreated (GrF) and treated (GrF-ZnO-TiO₂) anode substrate was investigated in the absence of applied current ($I = 0$) at 20 °C. Dye concentration decreased slightly during the first 20 min and then remained constant on the GrF. About 20 % of initial dye was adsorbed on the GrF at 20 min showing a moderate affinity of AB10B molecules for GrF substrate. In the case of

Fig. 5 Effect of applied current intensity on the degradation kinetics of AB10B (a) and kinetic analysis following pseudo first-order reaction (b). $[\text{dye}]_0 = 0.12 \text{ mM}$, $[\text{Fe}^{2+}] = 0.1 \text{ mM}$, $[\text{Na}_2\text{SO}_4] = 60 \text{ mM}$, $\text{pH} = 3$, temperature = $20 \pm 1 \text{ }^\circ\text{C}$

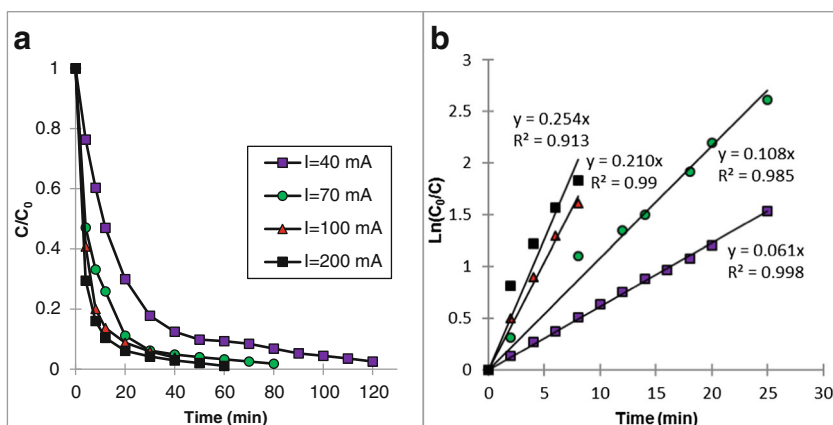


Table 1 Apparent rate constant (k_{app}) values as a function of the applied current intensity

I (mA)	40	70	100	200
k_{app} (min ⁻¹)	0.06	0.11	0.21	0.25
R ²	0.998	0.985	0.99	0.913

GrF-ZnO-TiO₂, adsorption of the dye was slow but continues during 60 min. It is worthy to notice that there is not accumulation of dye molecules on the anode surface during electrooxidation process since they are oxidized by M (\cdot OH) as they arrive on the surface (data not shown).

On the other hand, comparative experiments were carried out in ambient light, and in the dark showed that AB10B is not photosensitive and remains stable in solution during experiments. Therefore, the degradation of AB10B can be attributed to hydroxyl radicals (\cdot OH/M (\cdot OH)) generated in EAOPs (anodic oxidation and electro-Fenton).

Mineralization of AB10B aqueous solution

Oxidative degradation of an organic compound can lead to the formation of more toxic stable intermediates and thus increases the toxicity of the treated solution (Oturán et al. 2008; Dirany et al. 2012). Therefore, when applying advanced oxidation techniques, reaching an appreciable mineralization degree is essential to remove toxicity and form biodegradable and/or mineral end-products. To determine mineralization efficiency of different anodes tested in this study, TOC removal of 200 mL of 0.12 mM (74 mg L⁻¹) AB10B solution (corresponding to 31.7 g C L⁻¹) was investigated at 100 mA constant current. Three different sets of experiments were carried out with three different anodes, namely, GrF, GrF-ZnO-TiO₂, and stainless steel versus graphite felt cathode. Comparative TOC removal degree as mineralization efficiency for each tested anode was depicted in Fig. 7. In all cases, TOC removal kinetic

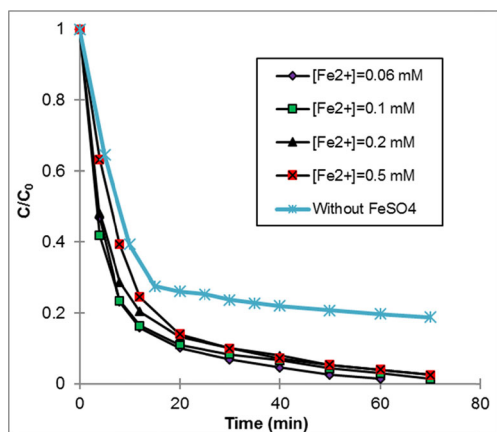


Fig. 6 Effect of Fe²⁺ concentration as catalyst on the degradation of AB10B at 100 mA constant current density. [AB10B]₀ = 0.12 mM, [Na₂SO₄] = 60 mM, [Fe²⁺]₀ = 0.1 mM, and room temperature (20 ± 1 °C)

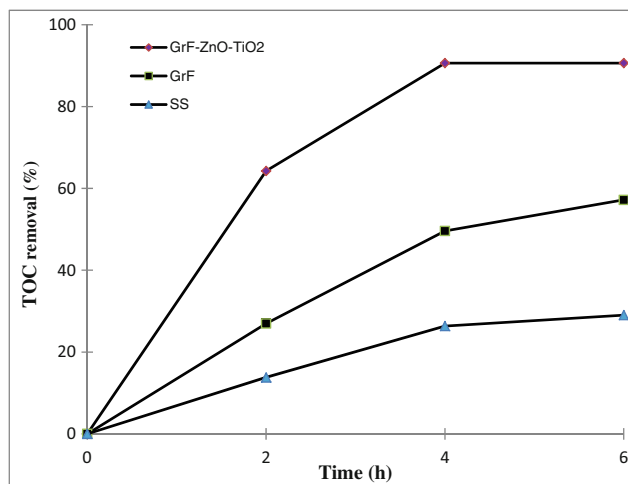


Fig. 7 TOC decay as mineralization efficiency during electrooxidation of AB10B dye aqueous solutions with GrF, SS steel, and GrF-ZnO-TiO₂ anodes. I = 100 mA, [Fe²⁺] = 0.1 mM, [AB10B]₀ = 0.12 mM, pH = 3, and room temperature (20 ± 1 °C)

was faster in the beginning of the treatment and decreased along the time and became poor at longer treatment time. This behavior is in agreement with the literature on the treatment of dyes or other organic pollutants by EAOPs (Lahkimi et al. 2007; Brillas et al. 2009; Olvera-Vargas et al. 2014; Brillas and Martínez-Huitle 2015). The decolorization of the solution occurred after 1 h treatment (as shown in Fig. 8) whereas the TOC removal was about 65 %. The TOC removal degree (removal percentage of initial solution TOC) after 6 h treatment was 29, 57, and 91 % for SS, GrF, and GrF-ZnO-TiO₂ anodes, respectively. These results highlight the poor mineralization power of SS anode (quasi absence of M (\cdot OH) generation on the anode) and high TOC removal power of GrF-ZnO-TiO₂ anode. In this latter case, the mineralization is quasi—almost complete. The residual solution TOC is formed mainly of short chain carboxylic acids which are hardly oxidized by \cdot OH (bulk) or M (\cdot OH)

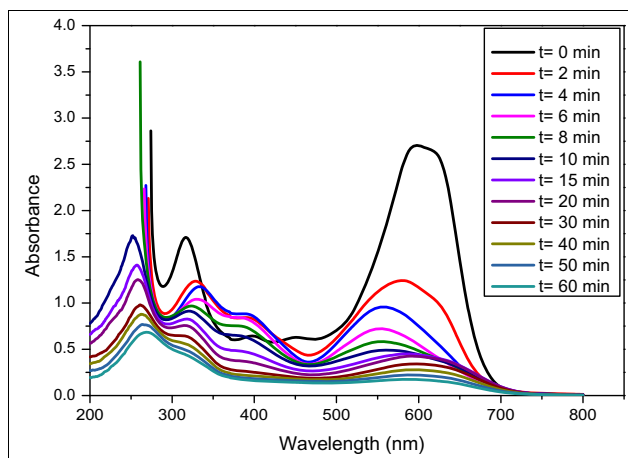


Fig. 8 UV-Vis spectral changes of AB10B dye (from t = 0 min to t = 60 min). Operating conditions: I = 100 mA, [AB10B]₀ = 0.12 mM, [Fe²⁺]₀ = 0.1 mM, pH = 3, [Na₂SO₄] = 60 mM, and temperature = 20 ± 1 °C

(anode surface) (Brillas et al. 2009; Diagne et al. 2014, Oturan and Aaron 2014). The above results highlight the great mineralization efficiency of GrF-ZnO-TiO₂ thin film anode on GrF substrate in treatment of AB10B solutions. This result can also be extrapolated to the treatment of other dye containing effluents.

Spectral changes of AB10B during electrooxidation experiments

The change in absorption spectra of AB10B solution as a function of the treatment time is shown in Fig. 8. As can be seen from this figure, UV-Vis spectrum of AB10B is characterized by one band in the visible region at 617 nm and two bands in the ultraviolet region at 226 and 318 nm. The results of this figure are in agreement with that already observed by Dinesh et al. 2014. The peak at 617 nm was attributed to the absorption of the $n \rightarrow \pi^*$ transition related to the $-N=N-$ group and the peaks at 226 and 318 nm were ascribed to the absorption of the $\pi \rightarrow \pi^*$ transition related to aromatic rings bonded to the $-N=N-$ group in the dye molecule (Dinesh et al. 2014; Solozhenko et al. 1995).

It was clearly observed that the peak centered at 617 nm decreased very fast leading to the disappearance of the UV band and a complete discoloration of the dye solution at 60 min electrolysis. In contrast to the absorption band at 226 and 318 nm, corresponding $\pi \rightarrow \pi^*$ transition are remaining at the end of 60 min treatment. That means the presence of some residual compounds with aromatic ring at this stage of the electrolysis. The complete destruction of these compounds requires more time as shown by TOC evolution of the solution (Fig. 7). Overall, these results confirm the quick AB10B concentration decay observed on Figs. 4, 5, and 6 and the fast discoloration of the solution during electrooxidation of the dye (Figs. 5 and 6).

Conclusions

From the results presented above, we can withdraw the following main conclusions:

- Electrochemical degradation of the diazo dye AB10B was investigated by electrochemical oxidation under several operating conditions including nature of electrodes (anode and cathode), current intensity, catalyst nature and concentration, and better degradation efficiency were obtained under the following operating conditions: GrF-ZnO-TiO₂ anode, 100 mA current intensity, and 0.1 mM Fe²⁺ (catalyst) concentration for 0.12 mM initial dye concentration.
- Discoloration of AB10B dye solution occurred, under these optimal experimental conditions, at 1 h electrolysis

while solution TOC removal was 65 % of its initial value in this stage of treatment. Therefore, almost mineralization degree (>91 % TOC removal) was reached at 6 h treatment with GrF-ZnO-TiO₂ composite thin film anode that seems to be the most powerful electrode for an efficient removal of AB10B dye from water.

References

- Aboul-Gheit AK, El-Desouki DS, El-Salamony RA (2014) Different outlet for preparing nano-TiO₂ catalysts for the photodegradation of Black B dye in water. *Egypt J Pet* 23:339–348
- Arslan I, Balcioglu IA, Bahnermann DV (2000) Advanced chemical oxidation of reactive dyes in simulated dyehouse effluents by ferrioxalate-Fenton/UV-A and TiO₂/UV-A processes. *Dyes Pigments* 47:207–218
- Brillas E, Martínez-Huitle CA (eds) (2011) Synthetic diamond films: preparation, electrochemistry, characterization, and applications. Wiley, New Jersey
- Brillas E, Martínez-Huitle CA (2015) Decontamination of wastewaters containing synthetic organic dyes by electrochemical methods. An updated review. *Appl Catal B Environ* 166:603–643
- Brillas E, Sirés I, Oturan MA (2009) Electro-Fenton process and related electrochemical technologies based on Fenton's reaction chemistry. *Chem Rev* 109:6570–6631
- Chung KT (2015) Occurrence, uses, and carcinogenicity of arylamines. *Front Biosci* 7:322–345
- de Araujo DM, Canizares P, Martínez-Huitle CA, Rodrigo MA (2014) Electrochemical conversion/combustion of a model organic pollutant on BDD anode: role of sp(3)/sp(2) ratio. *Electrochem Comm* 47: 37–40
- de Araujo DM, Saez C, Martínez-Huitle CA, Canizares P, Rodrigo MA (2015) Influence of mediated processes on the removal of Rhodamine with conductive-diamond electrochemical oxidation. *Appl Catal B-Environ* 166:454–459
- Diagne M, Sharma VK, Oturan N, Oturan MA (2014) Depollution of indigo dye by anodic oxidation and electro-Fenton processes using boron-doped diamond anode. *Environ Chem Lett* 12:219–224
- Dinesh VP, Biji P, Ashok A, Dhara SK, Kamruddin M, Tyagi AK, Raj B (2014) Plasmon-mediated, highly enhanced photocatalytic degradation of industrial textile dyes using hybrid ZnO@Ag core-shell nanorods. *RSC Adv* 4:58930–58940
- Dirany A, Sirés I, Oturan N, Özcan A, Oturan MA (2012) Electrochemical treatment of Sulfachloropyridazine: kinetics, reaction pathways, and toxicity evolution. *Environ Sci Technol* 46: 4074–4082
- El-Ghenymy A, Rodríguez RM, Brillas E, Oturan N, Oturan MA (2014) Electro-Fenton degradation of the antibiotic sulfanilamide with Pt/carbon-felt and BDD/carbon-felt cells. Kinetics, reaction intermediates and toxicity assessment. *Environ Sci Pollut Res* 21:8368–8378
- Es-Souni M (2011) Coating for polymers, European patent nr. EP2707438 (<https://www.google.com/patents/EP2707438A1?cl=en>)
- Guivarch E, Trevin S, Lahitte C, Oturan MA (2003) Degradation of azo dyes in water by electro-Fenton process. *Environ Chem Lett* 1:39–44
- Hisaindee S, Meentani MA, Rauf MA (2013) Application of LC-MS to the analysis of advanced oxidation process (AOP) degradation of dye products and reaction mechanisms. *Trends Anal Chem* 49:31–44

- Kirupavasam EK, Raj GAG (2012) Photocatalytic degradation of Amido black-10B using nanophotocatalyst. *J Chem Pharm Res* 4:2979–2987
- Labiadh L, Oturan MA, Panizza M, Ben Hamadi N, Ammar S (2015) Complete removal of AHPS synthetic dye from water using new electro-Fenton oxidation catalyzed by natural pyrite as heterogeneous catalyst. *J Hazard Mater* 297:34–41
- Lahkimi A, Chaouch M, Oturan N, Oturan MA (2007) Removal of textile dyes from water by electro-Fenton process. *Environ Chem Lett* 5: 35–39
- Lin H, Wu J, Oturan N, Zhang H, Oturan MA (2016) Degradation of artificial sweetener saccharin in aqueous medium by electrochemically generated hydroxyl radicals. *Environ Sci Pollut Res* 23:4442–4453
- Martinez-Huitle CA, Quiroz MA, Comninellis C, Ferro S, De Battisti A (2004) Electrochemical incineration of chloranilic acid using Ti/IrO₂, Pb/PbO₂ and Si/BDD electrodes. *Electrochim Acta* 50:949–956
- Mirkhani V, Tangestaninejad S, Moghadam M, Habibi MH, Rostami-Vartooni A (2009) Photodegradation of aromatic amines by Ag-TiO₂ photocatalyst. *J Iran Chem Soc* 6:800–807
- Olvera-Vargas H, Oturan N, Aravindakumar CT, Sunil Paul MM, Sharma VK, Oturan MA (2014) Electro-oxidation of the dye azure B: kinetics, mechanism and by-products. *Environ Sci Pollut Res* 21:8379–8386
- Oturan MA (2014) Electrochemical advanced oxidation technologies for removal of organic pollutants from water. *Environl Sci Pollut Res* 21:8333–8335
- Oturan MA, Aaron JJ (2014) Advanced oxidation processes in water/wastewater treatment: principles and applications. A review. *Crit Rev Environl Sci Technol* 44:2577–2641
- Oturan N, Trajkovska S, Oturan MA, Couderchet M, Aaron JJ (2008) Study of the toxicity of diuron and its metabolites formed in aqueous medium during application of the electrochemical advanced oxidation process “electro-Fenton”. *Chemosphere* 73:1550–1556
- Oturan N, Brillas E, Oturan MA (2012) Unprecedented total mineralization of atrazine and cyanuric acid by anodic oxidation and electro-Fenton with a boron-doped diamond anode. *Environ Chem Lett* 10: 165–170
- Panizza M, Cerisola G (2009) Direct and mediated anodic oxidation of organic pollutants. *Chem Rev* 109:6541–6569
- Panizza M, Dirany A, Sirés I, Haidar H, Oturan N, Oturan MA (2014) Complete mineralization of the antibiotic amoxicillin by electro-Fenton with a BDD anode. *J Appl Electrochem* 44:1327–1335
- Qamar M, Saquib M, Muneer M (2005) Photocatalytic degradation of two selected dye derivatives, chromotrope 2B and Amido black 10B, in aqueous suspensions of titanium dioxide. *Dyes Pigments* 65:1–9
- Rocha JHB, Solano AMS, Fernandes NS, da Silva DR, Peralta-Hernandez JM, Martinez-Huitle CA (2012) Electrochemical degradation of Remazol red BR and Novacron blue C-D dyes using diamond electrode. *Electrocatalysis* 3:1–12
- Rodrigo MA, Oturan N, Oturan MA (2014) Electrochemically assisted remediation of pesticides in soils and water: a review. *Chem Rev* 11: 8720–8745
- Sen S, Demirel GN (2003) Anaerobic treatment of real textile wastewater with a fluidized bed reactor. *Water Res* 37:1868–1878
- Senthilkumar S, Perumalsamy M, Janardhana Prabhu H (2014) Decolourization potential of white-rot fungus *Phanerochaete chrysosporium* on synthetic dye bath effluent containing Amido black 10B. *J Saudi Chem Soc* 18:845–853
- Shukla S, Oturan MA (2015) Dye removal via electrochemistry and oxidation using semiconductor oxides nanotubes. *Environ Chem Lett* 13:157–172
- Sirés I, Brillas E, Oturan MA, Rodrigo M, Panizza M (2014) Electrochemical advanced oxidation processes: today and tomorrow. A review. *Environ Sci Pollut Res* 21:8336–8367
- Solozhenko EG, Soboleva NM, Goncharuk VV (1995) Decolourization of azodye solutions by Fenton’s oxidation. *Water Res* 29:2206–2210
- Sun JH, Sun SP, Wang GL, Qiao L (2007) Degradation of azo dye Amido black 10B in aqueous solution by Fenton oxidation process. *Dyes Pigments* 74:647–652
- Tan KB, Vakili M, Hord BA, Poh PE, Abdullah AZ, Salamatinia B (2015) Adsorption of dyes by nanomaterials: recent developments and adsorption mechanisms. *Separ Purif Technol* 150:229–242
- Toh YC, Yen JLL, Obbard JP, Ting YP (2003) Decolourisation of azo dyes by white-rot fungi (WRF) isolated in Singapore. *Enzym Microb Technol* 33:569–575
- Vasudevan S, Oturan MA (2014) Electrochemistry: as cause and cure in water pollution—an overview. *Environ Chem Lett* 12:97–108